Micromechanics of Fracture in Notched Samples of Heavily Drawn Steel

J. Toribio[1] and F. J. Ayaso[2]

[1] Department of Materials Engineering, University of Salamanca, Spain
[2] Department of Materials Science, University of La Coruña, Spain

ABSTRACT: This paper deals with the influence of the manufacturing process on the microscopic fracture behaviour of axisymmetric notched specimens of pearlitic steels with different degrees of cold drawing. To this end, samples from different steps of the manufacturing chain were obtained, from the initial hot rolled material (not cold draw at all) to the final prestressing steel (heavily cold drawn). A detailed fractographic analysis was performed by using scanning electronic microscopy and image analysis techniques, in order to define and measure the fracture process zone in each case. Results show that the microscopic fracture modes range from ductile micro-void coalescence to brittle cleavage, depending on the stress triaxiality generated in the vicinity of the notch tip. A special fibrous region was detected, which allows a definition of the fracture process zone as the central region of the fractured area in bluntly notched samples and the external ring (i.e., the notch tip) in sharply notched specimens..

INTRODUCTION

Cold drawn eutectoid steels are structural materials of the greatest interest in civil engineering because they are frequently used in the form of wires and cables in prestressed concrete which usually works under very high stress levels and surrounded by harsh environments. The manufacturing process consists of cold drawing a previously hot rolled bar in order to increase the yield strength by means of a strain hardening mechanism.

Such a heavy drawing (with its associated plastic deformation) produces important microstructural changes in the steels [1-6] so that their macroscopic characteristics are seriously affected. As the final aim of manufacturing, classical mechanical properties such as the yield strength and the ultimate tensile stress are improved with cold drawing [7-9]. In addition, microstructural changes also affect (in a less clear manner) the fracture behaviour in air [10] and in aggressive environments [11], and the consequences are far from being totally understood.

This paper analyses the fracture micromechanisms in notched samples of progressively drawn pearlitic steels, in order to elucidate the microscopic topographies and the fracture process zone (FPZ) in the different materials under several stress triaxiality conditions provided by notches of very distinct geometries.

EXPERIMENTAL PROGRAMME

Materials and effect of cold drawing

The materials used in this research were high-strength eutectoid steels with seven different levels of cold drawing from a hot rolled bar (not cold drawn at all) to the commercial prestressing steel wire (heavily cold drawn). The main characteristics are given in another paper in these Proceedings [12]. Figure 1 shows a plot of the stress-strain curves of the different steels.
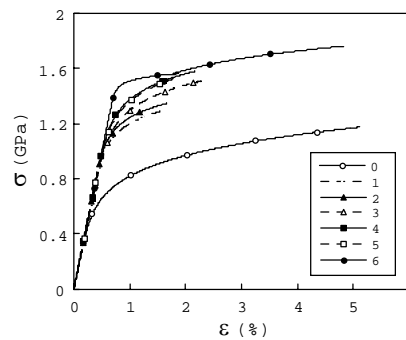
Figure 1: Stress-strain curves of the different steels.

Notched specimens

Axisymmetric notched specimens with a circumferentially-shaped notch were used in the experiments. Four notch geometries were used with each material, in order to achieve very different stress states in the vicinity of the notch tip and thus very distinct *constraint* situations, thus allowing an analysis of the influence of such factors on the micromechanical fracture processes. The dimensions of the specimens named A, B, C and D throughout this paper were the following:
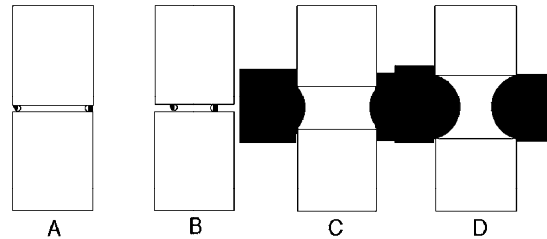
Geometry A : R/D = 0.03, C/D = 0.10
Geometry B : R/D = 0.05, C/D = 0.30
Geometry C : R/D = 0.40, C/D = 0.10
Geometry D : R/D = 0.40, C/D = 0.30

where R is the notch radius, C the notch depth and D the external diameter of the specimen. These four geometries are depicted in Figure 2.

**Figure 2:** Notched specimens used in the experimental programme.

Fracture tests

Three fracture tests were performed for each material and geometry (thus a total number of 84 tests were performed: seven materials, four notched geometries and three tests of each) recording continuously the load and the relative displacement between two points distant 25 mm. All the tests were performed under displacement control, so as to allow a complete recording of the load-displacement plot up to final failure, even in the case of ductile behaviour with prolonged decrease in load for increasing displacement.

EXPERIMENTAL RESULTS

Figure 3 shows the experimental results in the form of load *vs.* displacement for the representative test of each group of three (that displaying the intermediate curve). In the name of the specimens, the first symbol (the digit) indicates the steel (number of cold drawing steps) whereas the second symbol (the letter) denotes the notch geometry (A, B, C or D). The plots are represented using dimensionless variables F* and u* defined as $F^* = F / (\sigma_{02} S)$ and $u^* = u / d$, where F is the load applied on the sample during the fracture test, σ_{02} is the yield strength of each material, S the area of the net transversal section in the notched specimens, u the displacement recorded by the extensometer (corrected to obtain a constant ratio between the measurement distance and the different diameters of the steel wires) and d the minimum diameter of the notched samples ($S = \pi d^2/4$).

The procedure for obtaining dimensionless variables makes the curves fit into the same experimental bands with the exceptions of steels 0 and 6 due to the fact that their stress strain curves (cf. Fig. 1) have a shape which is slightly different from the others.
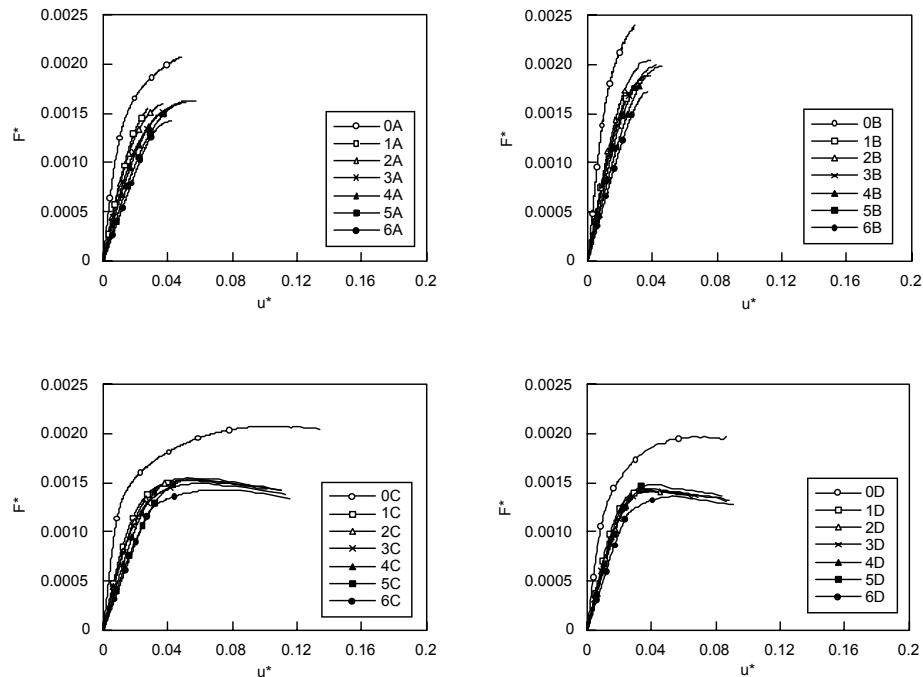
Figure 3: Load-displacement curves (dimensionless variables).

The shape of the F*-u* curves is dependent *only* of the notch geometry, i.e., of the *stress triaxiality* (or *mechanical constraint*), but not on the particular constitutive behaviour of each steel given in Fig. 1. Geometries A and B (sharp notch) present a macroscopically brittle fracture behaviour (with no evidence of load decrease), while in geometries C and D (blunt notch) the fracture behaviour is ductile, associated with a clear decrease in load in the F-u curves. The most brittle fracture behaviour (in macroscopic terms) is that of geometry B which has the highest level of constraint (i.e., maximum stress triaxiality).

FRACTOGRAPHIC ANALYSIS

A fractographic study by scanning electron microscopy (SEM) was performed on the fracture surfaces after the tests. Figure 4 shows the fractographs for notched specimens 0A (representative of sharp notch geometries A and B) and 0C (representative of blunt notch geometries C

and D). An aspect which can be distinguished by simple visual inspection is the presence of a shear lip in the vicinity of the notch tip, very clear in notched geometries C y D, specially in the latter. In the geometries A and B the shear lip is smaller, specially in the former ones. In the whole fracture area, the shear lip has a circumferential ring shape, i.e., it occupies in general the total periphery of the circle marking the notch tip in the axisymmetric samples. At the microscopic level, such a external ring is constituted by micro-void coalescence (MVC).
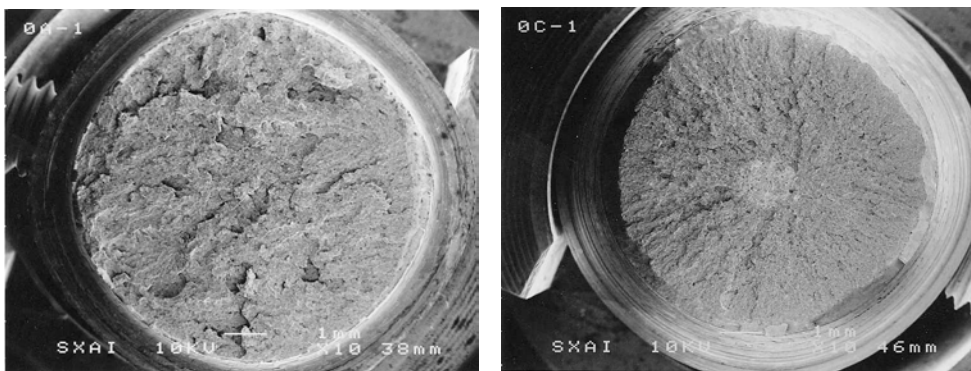
Figure 4: Fractographic appearance in specimens 0A and OC.

According to previous reasoning and from the microscopic point of view, geometries C and D with the biggest notch radius behave in a more ductile manner than geometries A and B, which is consistent with their macroscopic behaviour (load-displacement plots) described in the previous section of the paper, and the load decrease is associated with the more ductile behaviour in the bluntly notched geometries.

Geometries C and D exhibit a central fracture area with fibrous aspect and different colour and texture than those of the rest of the fracture area. Fracture initiates in such a central core with fibrous appearance, from which radial marks start towards the sample surface (notch tip), thus indicating the fracture propagation direction from the nucleus to the periphery. The microscopic appearance of the radial fracture area is cleavage (C).

Therefore, three different fracture regions may be distinguished: (i) an external ring formed by MVC which appears in all geometries; (ii) an intermediate zone, also detectable in all geometries, in which the presence of cleavage (C) is predominant, the size of this zone being smaller as the degree of cold drawing in the steel increases; (iii) a central fibrous zone which appears only in geometries C and D as a consequence of the very intense plastic deformation.

FRACTURE PROCESS ZONE

The final aim of this paper is the establishment of the fracture process zone (FPZ) in the notched samples of progressively drawn steels. To this end, a clarification is required of the specific features of the distinct MVC areas for the different triaxiality levels generated by the notches.

As mentioned above in general terms, the specimens with blunt notch (geometries C and D) exhibit a central fracture area of fibrous aspect, detectable by simple visual inspection At a higher magnification, the microscopic appearance of such a zone is shown in Figure 5(a). This fibrous area is formed mainly by MVC with some isolated cleavage regions which can also be detected. Such a special feature will be named MVC* throughout this paper, and it can be considered as the FPZ in notched geometries C and D, since fracture initiates in that fibrous MVC* region and propagates in unstable manner and radial direction by cleavage (C) towards the periphery of the specimens, as sketched in Figure 5(b).


(a)   (b)
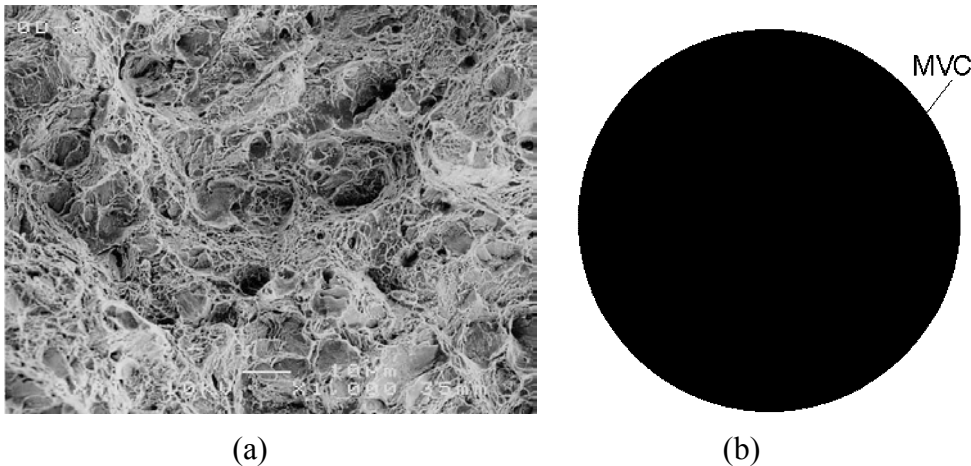
Figure 5: (a) Fracture by MVC* in the central fibrous region of sample 0D; (b) Initiation and propagation of fracture in notched geometries C and D.

With regard to the sharp notch specimens A and B, the FPZ must be located in the external ring, i.e., in the vicinity of the notch tip (due to the very high stress triaxiality levels there), and specifically in a region of the same in which the fractographic appearance is also MVC* (similarly to blunt notched geometries C and D, since the fracture initiation micromechanisms should be dependent only on the specific steel and not on the particular notched geometry). To check this item, a very detailed SEM

fractographic analysis was performed on samples A and B to find out whether or not such a MVC* topography could be observed anywhere. The analysis was successful, and thus some local MVC* regions were detected, with the appearance of Figure 5 (a). Thus the local MVC* region is the FPZ, associated with fracture initiation, in samples A and B, while the standard MVC ring is the final fracture area in those geometries, in the same manner as the cup and cone fracture type in a conventional tension test.

Figure 6 shows a sketch of the initiation and propagation of fracture in specimens A and B. The FPZ is bigger in samples with geometry A than in those with notch geometry B, sue to the higher triaxiality level in the latter. The higher the maximum stress triaxiality created by the notch, the lower the depth of the FPZ in the vicinity of the notch tip. The elevated stress triaxiality in geometry B also explains why in this case there are several initiation sites for fracture (multiple cleavage origins) at a certain distance from the notch tip, in contrast with the single cleavage origin in geometry A.

(a)   (b)
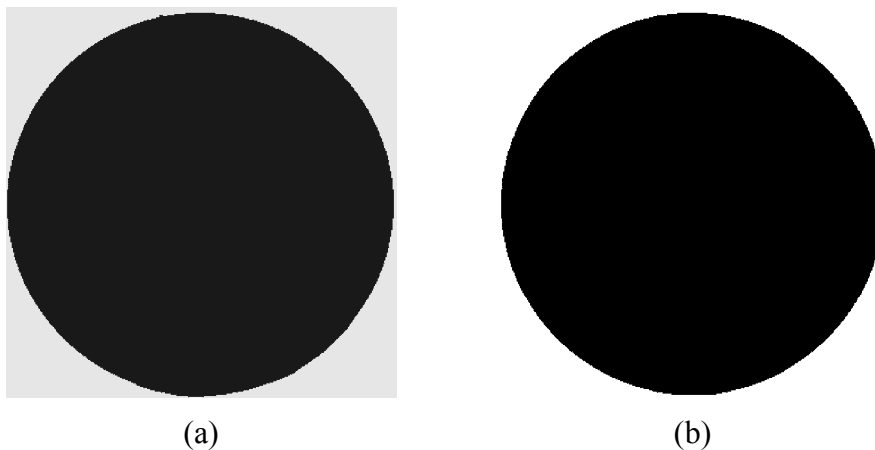
Figure 6: Initiation and propagation of fracture: (a) notched geometry A; (b) notched geometry B.

CONCLUSIONS

The fracture micromechanisms in notched samples of progressively drawn steels were analysed. The two predominant fractographic modes were ductile micro-void coalescence (MVC) and brittle cleavage. The locations and proportions of both topographies depend on the stress triaxiality (constraint) generated by the notch and on the degree of cold drawing.

Notched geometries A and B exhibit peripheral fracture initiation from an external MVC ring (at local areas with MVC*) and cleavage propagation towards the inner points, whereas geometries C and D show a central fracture initiation (fibrous zone by MVC*), radial cleavage propagation towards the periphery and final cup and cone fracture in the external ring.

Both the external ring in geometries A and B and the fracture core and the external ring in geometries C and D are constituted by MVC fractography, but the general features of the topography and the size of micro-voids is different from one to another. The micro-voids are bigger and the aspect more fibrous (MVC*) in the core of samples C and D and in local areas of the external ring in specimens A and B.

The above considerations allow a definition of the area in which fracture initiates or fracture process zone (FPZ) as the external ring by MVC (with local areas by MVC*) in sharp notch geometries A and B (brittle fracture behaviour), or as the central fibrous region (exclusively formed by MVC*) in blunt notch specimens C and D (ductile fracture behaviour).

REFERENCES

1. Embury, J.D. and Fisher, R.M. (1966) *Acta Metallurgica* **14**, 147.
2. Langford, G. (1970) *Metallurgical Transsactions* **1**, 465.
3. Toribio, J. and Ovejero, E. (1997) *Materials Science and Engineering* **A234-236**, 579.
4. Toribio, J. and Ovejero, E. (1998) *Journal of Materials Science Letters* **17**, 1037.
5. Toribio, J. and Ovejero, E. (1998) *Scripta Materialia* **39**, 323.
6. Toribio, J. and Ovejero, E. (1998) *Mechanics of Time-Dependent Materials* **1**, 307.
7. Hyzak, J.M. and Bernstein, I.M. (1976) *Metallurgical Transactions* **7A**, 1217.
8. Kavishe, F.P.L. and Baker, T.J. (1986) *Materials Science and Technology* **2**, 816.
9. Alexander, D.J. and Bernstein, I.M. (1989) *Metallurgical Transactions* **20A**, 2321.
10. Toribio, J. (2002) *ISIJ International*, in press.
11. Toribio, J. and Lancha, A.M. (1996) *Journal of Materials Science* **31**, 6015.
12. Toribio, J., Ayaso, F.J. and Ovejero, E. (2002) *Proceedings of the 14th European Conference on Fracture-ECF14*, in press.